JACS
JOURNAL OF THE AMERICAN CHEMICAL SOCIETY

COMMUNICATION

pubs.acs.org/JACS

Photocatalytic Water Oxidation with Nonsensitized IrO_2 Nanocrystals under Visible and UV Light

F. Andrew Frame,[†] Troy K. Townsend,[†] Rachel L. Chamousis,[†] Erwin M. Sabio,[†] Th. Dittrich,[‡] Nigel D. Browning,[§] and Frank E. Osterloh*[,†]

[†]Department of Chemistry, University of California, Davis, One Shields Ave, Davis, California 95616, United States

[‡]Helmholtz-Zentrum Berlin für Materialien und Energie, Hahn Meitner Platz 1, D-14109 Berlin, Germany

[§]Department of Chemical Engineering and Materials Science, University of California, Davis, One Shields Avenue, Davis, California 95616, United States

Lawrence Livermore National Laboratory, 7000 East Avenue, Livermore, California 94550, United States

Supporting Information

ABSTRACT: Rutile IrO_2 is known as being among the best electrocatalysts for water oxidation. Here we report on the unexpected photocatalytic water oxidation activity of 1.98 nm ± 0.11 nm succinic acid-stabilized IrO_2 nanocrystals. From aqueous persulfate and silver nitrate solution the nonsensitized particles evolve oxygen with initial rates up to 0.96 μmol min^{-1}, and with a quantum efficiency of at least 0.19% (measured at 530 nm). The catalytic process is driven by visible excitations from the Ir-d(t_{2g}) to the Ir-d(e_g) band (1.5−2.75 eV) and by ultraviolet excitations from the O-p band to the Ir-d(e_g) (>3.0 eV) band. The formation of the photogenerated charge carriers can be directly observed with surface photovoltage spectroscopy. The results shed new light on the role of IrO_2 in dye- and semiconductor-sensitized water splitting systems.

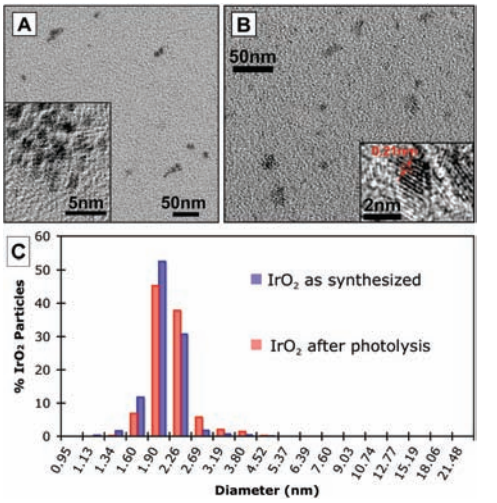

Figure 1. (A) Low- and high-resolution TEMs (inset) of succinate-capped IrO_2 nanocrystals. (B) Low- and high-resolution TEMs (inset) of IrO_2 nanocrystals after oxygen evolution reaction. (C) Dynamic light scattering (DLS) measurement of IrO_2 colloid. Shown are as-synthesized and post-photolysis materials in basic solutions.

Because IrO_2 has a very low electrochemical overpotential for water oxidation,[1−6] it is widely used in commercial water electrolyzers and as a cocatalyst in photochemical water splitting devices. In these systems, which convert abundant solar energy into renewable hydrogen fuel, IrO_2 is usually connected to a light absorber, e.g. an inorganic semiconductor[7−10] or a molecular dye.[4,11−15] Upon optical excitation, the light absorber funnels holes to the IrO_2 component to facilitate water oxidation, whereas electrons are absorbed by an electrode or by a sacrificial acceptor. Here, we report the unexpected finding that ∼2.00-nm succinate-stabilized IrO_2 nanocrystals photocatalyze oxygen formation from aqueous solutions of sacrificial electron acceptors, without the use of an external light absorber. Using surface photovoltage spectroscopy, we show that photochemical charge carriers are formed when electrons are excited from the Ir-d(t_{2g}) to the Ir-d(e_g) band (1.5−2.75 eV) or from the O-p to the Ir-d(e_g) band (>3.0 eV). Such a photocatalytic function has not been previously observed for IrO_2.

Succinate-capped IrO_2 nanocrystals were synthesized by hydrolysis of an aqueous potassium hexachloroiridate (IV) solution according to the procedure by Hoertz et al.[15] TEM measurements (Figure 1A) show crystalline particles (1.98 nm ± 0.11 nm) with measured lattice row spacing of 0.21 nm ± 0.01 nm, corresponding to the 001 lattice plane. On the TEM grid, the particles are aggregated into clusters with diameters between 20 and 40 nm.

Dynamic light scattering (DLS) performed directly on the sol shows a narrow particle distribution as seen in Figure 1C. As expected, the hydrodynamic radius of the particles (2.19 nm ±0.13 nm) is slightly larger than the radius determined by TEM. There is no detectable quantity of particle aggregation in solution by DLS. Thus, the clusters seen by TEM are a drying artifact.

The IrO_2 sol has a characteristic blue appearance due to a broad absorption band centered at 570 nm. This band is due to transitions between t_{2g} and e_g orbitals of an Ir^{4+} ion in a distorted octahedral coordination environment, whereas the absorption below 400 nm (Figure 2A) is associated with a O-p to Ir-d ligand-to-metal charge transfer process.[15−17] These transitions are also shown in the energy scheme in Figure 3C.

Received: January 6, 2011
Published: April 27, 2011

dx.doi.org/10.1021/ja200144w | J. Am. Chem. Soc. 2011, 133, 7264–7267

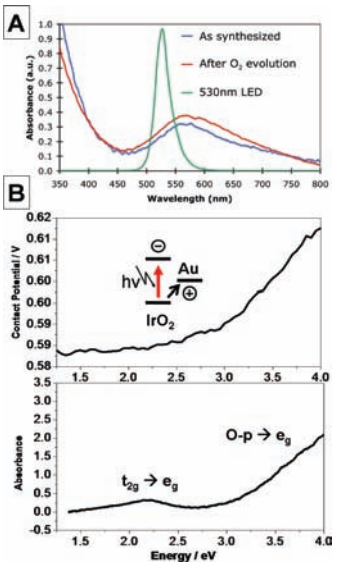

Figure 2. (A) UV−vis spectra of IrO_2 colloid as synthesized and after oxygen evolution reaction in sodium persulfate solution. Also shown is the spectrum of the 530 nm LED used for quantum efficiency measurements. (B) Surface photovoltage spectrum of IrO_2 nanoparticle film on Au substrate with illumination from Xe lamp (upper spectrum) and optical absorbance vs photon energy (lower spectrum).

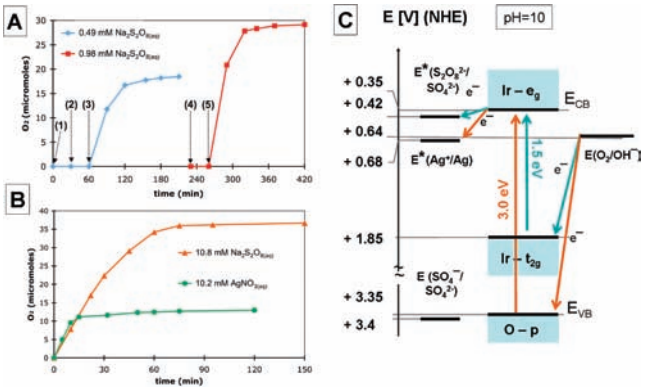

Figure 3. (A) O_2 evolution data for IrO_2 nanocrystals (3.7 mg) suspended in the 100 mL of solutions of sacrificial electron acceptors under visible (λ > 400 nm) irradiation (300 W Xe lamp). (1) light on, water (2) light off, 49.2 μmol $Na_2S_2O_{8(aq)}$ added; (3) light on; (4) light off, evacuated and backfilled with Ar, 98.4 μmol $Na_2S_2O_{8(aq)}$ added; (5) light on. (B) O_2 evolution from 10.8 mM $Na_2S_2O_8$ (λ>400 nm) and from 10.2 mM $AgNO_3$ (full spectrum). (C) Energy scheme for IrO_2, showing optical transitions and electron transfer processes. Reduction potentials E^* are calculated for 1.0 mM $Na_2S_2O_8$ and for 10.0 mM $AgNO_3$.

Surface photovoltage spectroscopy (SPV) gives information about electronic transitions from which charge separation can occur.[18] In SPV, a light-induced change of the contact potential of a sample is recorded as a function of the irradiation wavelength/energy. This allows one to observe the generation and separation of photochemical charge carriers in inorganic semiconductors.[19,20] The spectrum obtained for a IrO_2 nanocrystal film on a Au substrate is shown in Figure 2B (upper diagram). The initial contact potential is solely determined by the difference of work functions between the gold reference electrode and the IrO_2 film. A light-induced change of the contact potential difference (ΔCPD) sets on at photon energies between 2 and 2.5 eV. The sign of ΔCPD is positive, which indicates that holes are separated preferentially toward the Au substrate, leading to negative charge accumulation in the IrO_2 film (for diagram see inset in Figure 2B). As the photon energy is increased above 3.0 eV, the contact potential increases first slowly, and then more strongly. Comparison with the optical absorbance data of the IrO_2 film (bottom diagram) reveals that the low-energy SPV signal correlates with the d−d transition at 1.50−2.75 eV. The signal above 3.0 eV correlates with the absorption edge at 3.0 eV, which is due to a ligand-to-metal charge transfer (MLCT) transition from the O-p band to the Ir-e_g band. These transitions are also shown in the energy scheme in Figure 3C. In order to produce a SPV signal, charge carriers need to diffuse to the IrO_2−Au interface, so they can get separated. According to recent calculations, the IrO_2 valence band has contributions from oxygen 2s, 2p, and iridium 5d states, and the conduction band is made of iridium 5d orbitals.[17] Thus, there exist two separate paths for transport of charge carriers to the nanocrystal surface.

To probe if the photochemical charge carriers are able to drive a chemical reaction on the surface of the IrO_2 particles, irradiation tests were performed on aqueous IrO_2 sols in the presence of sodium persulfate and silver nitrate as sacrificial electron acceptors (for reaction details see Supporting Information [SI]). In the first experiment, an argon sparged and degassed IrO_2 sol (3.7 mg of IrO_2) at pH 10 was placed in the photoreactor. When the mixture was irradiated with visible light (point 1 in Figure 3A), no oxygen is produced. A 10 mL aliquot of degassed 4.92 mM $Na_2S_2O_{8(aq)}$ (49.2 μmol $S_2O_8^{-2}$) was then added, and the mixture was kept in the dark for 30 min to confirm that no O_2 evolution took place (point 2). At point 3, light (>400 nm) was turned on to induce O_2 formation at an initial rate of 0.39 μmol O_2 min^{-1}. The rate then declines to zero after 3.5 h. At that point the IrO_2 turnover number (TON) equals 1.12, and 75.0% of the persulfate has been consumed. To confirm that the IrO_2 is still catalytically active, the oxygen was removed in vacuum and another 20.0 mL aliquot of degassed 4.92 mM $Na_2S_2O_{8(aq)}$ (98.4 μmol) was added at point 4 with stirring, upon which no O_2 evolution took place for 30 min. At point 5 the lamp was turned on again, and O_2 was evolved at a rate of 0.69 μmol O_2 min^{-1}, nearly twice the previous rate. After 2 h the rate then decreased to almost zero, with the IrO_2 reaching TON = 1.76 after 7.0 h total experiment time (310 min total irradiation time). At that time, the pH was 7.9, and 59.2% of the added persulfate had been consumed.

To test the influence of the persulfate concentration, a third irradiation was performed on a fresh batch of IrO_2 in the presence of 10.8 mmol L^{-1} of persulfate adjusted with 0.1 M NaOH to an initial pH of 10 (Figure 3B). Even though the persulfate concentration was ~10 times higher than in the previous test, O_2 was evolved at 0.75 μmol min^{-1}, i.e. just slightly above the rate from before. This shows that the rate of O_2 evolution is not limited by the availability of sacrificial acceptor. When the irradiation was repeated using fresh catalyst under similar conditions using a high power LED (530 nm, 15.0 mW/cm^2, emission spectrum in Figure 2A), an apparent quantum efficiency of 0.19% was determined. This value represents a minimum estimate, because of the low absorption coefficient (at 530 nm) of IrO_2 and the low concentration of the sol.

Inspection of the irradiated IrO_2 sol with electron microscopy and dynamic light scattering revealed no significant changes in crystallinity and size (Figure 1B/C), or in the optical properties

dx.doi.org/10.1021/ja200144w |J. Am. Chem. Soc. 2011, 133, 7264–7267

(UV−vis spectrum in Figure 2A). These observations support a catalytic role of the material.

To determine the activity of the sol under UV light, additional irradiations (Figure 3B) were performed using silver nitrate as electron acceptor (sodium persulfate is unstable under UV irradiation). Again, no O_2 was evolved in the dark, but in the presence of UV/visible light, oxygen was evolved at an initial rate of 0.96 μmol of O_2 min^{-1}, even greater than the rate with persulfate (see Figure 3B). However, after 10 min the rate quickly declined to reach nearly zero after 2 h. At the end of the experiment the pH was 3.4, and the turnover number was 0.79. The fast rate decline and the low turnover number are attributed to the deposition of silver metal onto the surface of the IrO_2 nanocrystals, leading to blockage of sites involved in light absorption and redox reactions.[21]

To obtain insight into the energetics of catalytic oxygen evolution, electrochemical and photoelectrochemical experiments were conducted on films of electroflocculated IrO_2 nanocrystals. Dark scans (Figure S2A, SI) on IrO_2 films on an indium tin oxide electrode reveal an onset potential for water oxidation at +1.19 V (pH = 10, 0.5 mA cm^{-2}), corresponding to an overpotential of η_{ox} = +0.55 V (using $E(O_2/OH^-)$ = +0.64 V at pH = 10 as a reference). Thus, the succinate-capped IrO_2 nanocrystals appear slightly less effective than similarly made surfactant-free IrO_2 particles (η_{ox} = 0.25 V),[3] which is a likely consequence of succinate blocking active sites. Using anodic scans under chopped irradiation (Figure S2B, SI), the photo-onset potential of IrO_2 is found at +0.35 V (NHE). This potential is an estimate for the conduction band edge E_{CB} in IrO_2.[7,22,23] It is in reasonable agreement with the estimated value of E_{CB} = + 0.51 V (NHE) according to the method of Butler and Ginley (SI).[24,25]

The IrO_2 conduction band edge potential can be used to construct the energy scheme in Figure 3C (compare also Sorantin et al.[26]). Here the positions of the valence band edge E_{VB} and of the metal t_{2g} band edge follow from the optical bandgaps of 3.0 and 1.5 eV respectively. Values for the oxygen reduction potential and for silver ion and persulfate reduction potentials[27] are also listed, after correction for pH and concentrations. It can be seen that E_{VB} and the edge potential of the Ir-$t_{2\,g}$ band are sufficiently positive to oxidize water and E_{CB} is sufficiently negative to reduce the sacrifical acceptors. Thus, photocatalytic O_2 evolution can proceed either by visible excitation of electrons from the Ir-d (t_{2g}) band or by UV excitation of electrons from the O-p band into the metal Ir-d (e_g) band. The greater oxidation potential of the O-p band suggests that water oxidation under UV irradiation should be faster than under visible irradiation. This is indeed observed experimentally during the initial minutes of irradiation (Figure 3B). On the other hand, the greater rate might also be attributed to the more positive reduction potential of AgNO3 compared to that of persulfate (see below). Because at 1.0 mM concentration, the reduction potential for silver ion (+0.68 V) is at almost same position as the water oxidation potential at pH 10 (+0.64 V), oxygen formation with silver nitrate is nearly thermoneutral. Under these conditions IrO_2 acts as a photochemical diode that moves electrons from water to the electron acceptor. When persulfate is used as electron acceptor, the situation is more complicated. For persulfate a thermodynamic reduction potential of 2.01 V is tabulated in the literature.[27] However, persulfate accepts two electrons at two separate potentials.[28] The first reaction proceeds at +0.6 V, producing sulfate and a SO_4^- radical. The relatively low reduction potential for this reduction step is the reason why mixtures of sodium persulfate and IrO_2 particles do not spontaneously evolve O_2 in the dark, as we observe (Figure S1, SI, and dark periods in Figure 3A) and as others have noted.[4,7−15] The formed SO_4^- radical, on the other hand, is a strongly oxidizing agent (E^0 = +3.4 V) that could oxidize water with or without participation of IrO_2. While it is possible that direct water oxidation by SO_4^- contributes to the observed O_2, it is not required as a necessary step to explain O_2 evolution in the system. This is what the results with silver nitrate show.

In conclusion we have demonstrated that nonsensitized succinate-stabilized IrO_2 nanocrystals are active for photocatalytic O_2 evolution from aqueous persulfate and silver nitrate solutions with a quantum efficiency of at least 0.19% (at 530 nm) and turnover numbers above unity. The process is driven by visible excitations among Ir-d (t_{2g}) and the Ir-d(e_g) bands and by ultraviolet excitations from the O-p band into the Ir-d(e_g) band. Photocatalytic oxygen evolution is aided by low-lying valence bands at +3.35 V and +1.85 V and by a low overpotential for water oxidation (+0.55 V at 0.5 mA cm^{-2}). The photocatalytic activity of nano-IrO_2 is unusual, considering the metal-like electronic structure of this compound.[17] Even though the activity is very low, it should be considered in the design of water splitting systems that employ IrO_2 together with a sensitizer. Lastly, the results on nano-IrO_2 suggest that similar photocatalytic activity may also be found in nanocrystals of other transition metal oxides, whose valence and conduction band energies are comparable to those of IrO_2.

■ ASSOCIATED CONTENT

Supporting Information. Full experimental details, background oxygen evolution data, electrochemical data, and calculation of the flat band potential. This material is available free of charge via the Internet at http://pubs.acs.org.

■ AUTHOR INFORMATION

Corresponding Author
fosterloh@ucdavis.edu

■ ACKNOWLEDGMENT

We thank Stephanie R. Dungan (UC Davis) for use of their DLS instrument and the National Science Foundation (Grant 0829142) and the U.S. Department of Energy (Grant FG02-03ER46057) for financial support of this work. FEO thanks the DAAD (German Academic Exchange Service) for a Faculty Research Visit Grant.

■ REFERENCES

(1) Yagi, M.; Tomita, E.; Kuwabara, T. *J. Electroanal. Chem.* **2005**, *579* (1), 83.
(2) Hackwood, S.; Schiavone, L. M.; Dautremontsmith, W. C.; Beni, G. *J. Electrochem. Soc.* **1981**, *128* (12), 2569.
(3) Nakagawa, T.; Beasley, C. A.; Murray, R. W. *J. Phys. Chem. C* **2009**, *113* (30), 12958.
(4) Harriman, A.; Thomas, J. M.; Millward, G. R. *New J. Chem.* **1987**, *11*, 757.
(5) Mills, A.; Russell, T. *J. Chem. Soc., Faraday Trans.* **1991**, *87* (8), 1245.
(6) Morris, N. D.; Mallouk, T. E. *J. Am. Chem. Soc.* **2002**, *124* (37), 11114.

(7) Ishikawa, A.; Takata, T.; Kondo, J. N.; Hara, M.; Kobayashi, H.; Domen, K. *J. Am. Chem. Soc.* **2002**, *124* (45), 13547.
(8) Kasahara, A.; Nukumizu, K.; Hitoki, G.; Takata, T.; Kondo, J. N.; Hara, M.; Kobayashi, H.; Domen, K. *J. Phys. Chem. A* **2002**, *106* (29), 6750.
(9) Iwase, A.; Kato, H.; Kudo, A. *Chem. Lett.* **2005**, *34* (7), 946.
(10) Youngblood, W. J.; Lee, S. H. A.; Kobayashi, Y.; Hernandez-Pagan, E. A.; Hoertz, P. G.; Moore, T. A.; Moore, A. L.; Gust, D.; Mallouk, T. E. *J. Am. Chem. Soc.* **2009**, *131* (3), 926.
(11) Harriman, A.; Pickering, I. J.; Thomas, J. M.; Christensen, P. A. *J. Chem. Soc., Faraday Trans. I* **1988**, *84*, 2795.
(12) Harriman, A.; Nahor, G. S.; Mosseri, S.; Neta, P. *J. Chem. Soc., Faraday Trans. I* **1988**, *84*, 2821.
(13) Hara, M.; Mallouk, T. E. *Chem. Commun.* **2000**, *19*, 1903.
(14) Hara, M.; Waraksa, C. C.; Lean, J. T.; Lewis, B. A.; Mallouk, T. E. *J. Phys. Chem. A* **2000**, *104* (22), 5275.
(15) Hoertz, P. G.; Kim, Y. I.; Youngblood, W. J.; Mallouk, T. E. *J. Phys. Chem. B* **2007**, *111* (24), 6845.
(16) Goel, A. K.; Skorinko, G.; Pollak, F. H. *Phys. Rev. B* **1981**, *24* (12), 7342.
(17) de Almeida, J. S.; Ahuja, R. *Phys. Rev. B* **2006**, *73* (16), 165102.
(18) Kronik, L.; Shapira, Y. *Surf. Sci. Rep.* **1999**, *37* (1−5), 1.
(19) Gross, D.; Mora-Sero, I.; Dittrich, T.; Belaidi, A.; Mauser, C.; Houtepen, A. J.; Da Como, E.; Rogach, A. L.; Feldmann, J. *J. Am. Chem. Soc.* **2010**, *132* (17), 5981.
(20) Mora-Sero, I.; Bisquert, J.; Dittrich, T.; Belaidi, A.; Susha, A. S.; Rogach, A. L. *J. Phys. Chem. C* **2007**, *111* (40), 14889.
(21) Sabio, E. M.; Chi, M.; Browning, N. D.; Osterloh, F. E. *Langmuir* **2010**, *26* (10), 7254.
(22) Bard, A. J.; Faulkner, L. R. *Electrochemical Methods: Fundamentals and Applications*, 2nd ed.; John Wiley: New York, 2001; p 754.
(23) Akatsuka, K.; Takanashi, G.; Ebina, Y.; Sakai, N.; Haga, M.; Sasaki, T. *J. Phys. Chem. Solids* **2008**, *69* (5−6), 1288.
(24) Butler, M. A.; Ginley, D. S. *J. Electrochem. Soc.* **1978**, *125* (2), 228.
(25) Xu, Y.; Schoonen, M. A. A. *Am. Mineral.* **2000**, *85* (3−4), 543.
(26) Sorantin, P. I.; Schwarz, K. *Inorg. Chem.* **1992**, *31* (4), 567.
(27) Vanysek, P. *CRC Handbook of Chemistry and Physics*, 88th (Internet Version 2008) ed.; Lide, D. R., Ed.; Electrochemical Series, CRC Press/Taylor and Francis: Boca Raton, FL, 2008.
(28) Memming, R. *J. Electrochem. Soc.* **1969**, *116* (6), 785.